Journal of Structural Geology, Vol. 5, No. 1, pp. 33 to 45, 1983
Printed in Great Britain

0191-8141/83/010033-13 $03.00/0
Pergamon Press Ltd.

Displacement features associated with fault zones: a comparison between observed examples and experimental models

J. F. GAMOND

Equipe de Recherches Associée au C.N.R.S. n° 603, Institut de Recherches Interdisciplinaires de Géologie et de Mécanique, BP 53 X, 38041 Grenoble-cedex, France

(*Received* 8 *June* 1982; *accepted in revised form* 2 *November* 1982)

Abstract—Fault zones commonly consist of discontinuous surfaces or are composed of different kinds of en échelon fractures (tension cracks, R or P-type fractures) which give the brittle shear zone a width. Translation along these faults and related features can occur by sliding on the elementary planes and/or by solution/deposition processes with opening of transtension zones and possible dilatation of the shear zone.

In order to understand how fault planes develop and to investigate the mechanical conditions corresponding to natural configurations, displacement along an analogue fault model was examined under conditions of direct shear. The experimental fracture patterns were then compared with the natural features. The structural elements of certain faults created by testing, and showing transpression and transtension zones, were found to be similar to natural domino structures bounded by elementary shears, and could be compared with computed situations.

It can be inferred that stresses are reoriented inside the shear zone; the angle between elementary fractures depends on their order of development; transpression and transtension zones occur systematically; and the shear zone undergoes dilatancy under low normal stresses.

INTRODUCTION

THE IMAGE one has of an ordinary fault zone along which displacement has occurred is usually that of a grooved fault plane. The fault separates two rock bodies which have been displaced relative to each other with friction, but without apparent internal deformation. It is possible to determine the relative direction of translation from the grooves, and its sense and magnitude from the offset of markers on each side of the fault. However, in the field the discontinuity is rarely a single plane. Rather there is a zone containing elementary fractures of different types, for example arrays of en échelon tension cracks, Riedel shears (R and R′) and P fractures. These fractures result from shearing effective over a variable width on either side of the shear zone. Where this occurs there is a union of several types of elementary fractures and the overall direction of the shear zone is different from that of the individual segments. It is often difficult to ascertain the sense of the translation from the associated elementary fractures and consequently the mechanical conditions giving rise to one association rather than another.

ELEMENTARY FRACTURES OF NATURAL SHEAR ZONES

Several types of fractures, which never occur all together, may be present in a given section of fault zone.

En échelon arrays of tension cracks (T)

It is generally supposed that tension cracks are parallel to the direction of the major principal stress (σ_1) in the shear zone. The angle which the tension cracks make with the shear plane is generally close to 45° (Hancock 1972, fig. 2, Vialon 1979, fig. 10), although values less than this have been reported (Delair 1977).

En échelon Riedel fractures (R and R′)

These fractures make an angle of $\pi/4 - \phi/2$ (ϕ = angle of internal friction of the rock) with the major principal stress in the interior of a shear zone (Wallace 1973, Fabre & Robert 1976). When dilatation is inhibited (Vialon 1979) the R fractures are more likely to develop than the R′.

En échelon P fractures

These fractures are symmetrical to the (R) fractures with respect to the shear direction, and are only thought to develop in the case where dilatation of the zone is possible (Vialon 1979), or where there has been substantial displacement (Tchalenko & Ambraseys 1970).

DECIMETRIC-SCALE STRUCTURES SHOWING AN ASSOCIATION OF DIFFERENT TYPES OF CRACKS

Dominoes

Many decimetric-scale shear zones are composed of two sets of fracture arrays, joined to each other, giving the appearance of a broken line or staircase. The sliding which occurs on one of the two sets, causes transform microfaults that allow the opening of the other set and the development of prismatic gaps (here called

dominoes) filled with quartz, chlorite or prehnite (Figs. 1–3). Where these minerals are fibrous the fibres are parallel to the relative displacement vector of the two wall rocks (Durney & Ramsay 1973, fig. 18, Spörli & Anderson 1980, figs. 2 and 3), that is parallel to the elementary fracture on which sliding occurs.

According to some current interpretations (e.g. Robert 1979) it is assumed that the fractures that opened to make the dominoes are tension cracks. It has also been proposed that the arrangement of the cracks in an array indicates the general direction of shear (e.g. Hancock 1972). The fractures which join them and allow

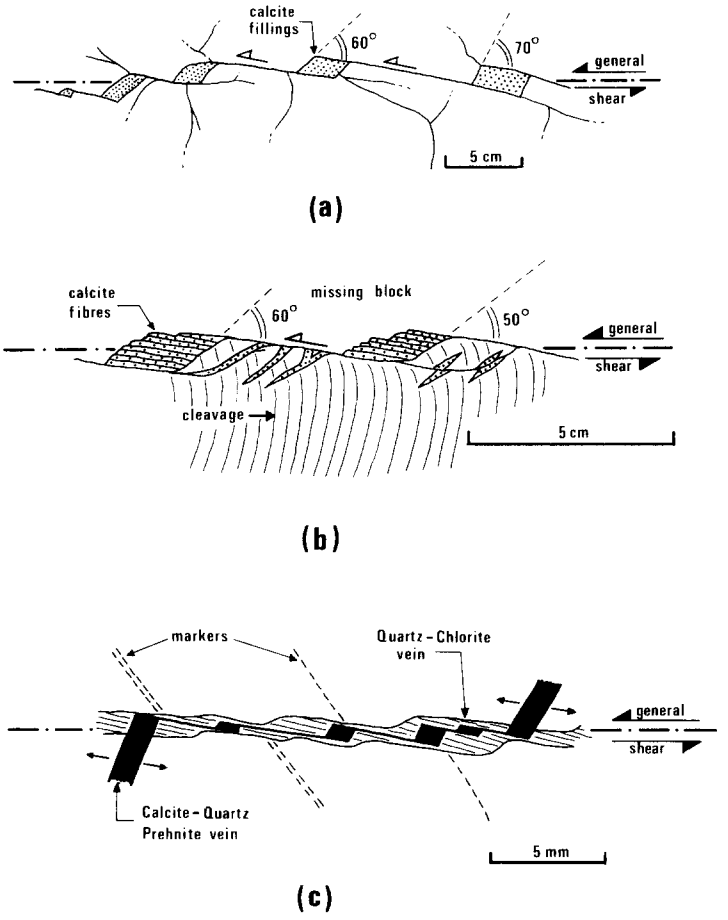

Fig. 1. Ordinary dominoes indicating relative left-lateral movement. (a) On the surface of a calcareous bed in the flysch of the côte Basque. (b) Transverse shear plane in a calcareous bed in the Dauphinois Dogger (road from Chevronnet to Allondaz, Savoie). Note the deformed cleavage near the shear plane. (c) Calcite–quartz–prehnite dominoes opened across an older quartz–chlorite filling of a staircase-like fracture.

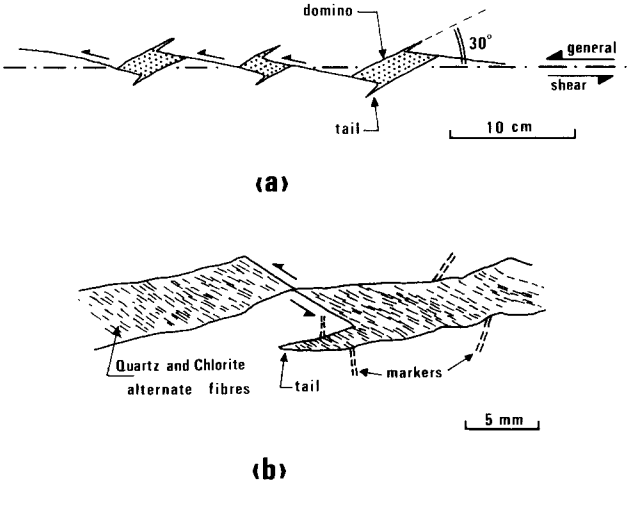

Fig. 2. Tailed dominoes defining a left lateral-shear. (a) Exposed on the surface of a calcareous bed in the flysch of the Côte Basque (after Robert 1979, fig. 145). (b) In argillite and chert mélange of the Auckland area. Alternating fibres of quartz and chlorite grew parallel to the transform microfault (after Spörli & Anderson 1980, fig. 2).

their opening may correspond to fractures of P Type. The oblique character of the second-generation fractures with respect to the general direction of shear has as a geometric consequence the dilatation of the shear zone (Fig. 4) (Wallace 1973, Vialon 1979, Spörli & Anderson 1980).

However these interpretations are not entirely satisfactory; extension cracks generally being considered to form at an angle of 45° to the direction of the shear. But, as the examples below show, this angle is commonly greater or less than 45° (Figs. 1–3; see also Hancock 1972); an alternative interpretation being proposed later. In addition, the most common dominoes are enclosed by an angle of 50–90° between the fracture which opens and that which slips (Fig. 1, Spörli & Anderson 1980, fig. 2b). The latter ordinarily forms a very small angle (10–20°) with the general direction of shear.

Furthermore, dominoes enclosed by angles of less than 45° contain fillings (Fig. 2, Bodou 1972, Robert 1979, Spörli & Anderson 1980, fig. 3) of prismatic form which are extended by a sharp crack in some places. There is in general an angle of 30° between the fracture that opens and that which slips, the latter being slightly oblique to the general alignment. Sliding causes the characteristic offset of the tails (Fig. 2) that indicates the sequence of fracture development.

An example observed in the External Crystalline Massif of the Grandes Rousses illustrates a special phenomenon (Fig. 3). The zone affects gneisses whose leucocratic layers serve as offset markers. The angle between the fractures which open and the general direction of shear is from 15 to 20°. The offset of the marker layers reaches a value d greater than the offset d' of the walls of the open fracture. Hence a decrease in volume must be admitted in the vicinity of the oblique sliding-fracture.

Wavy faults

The plane of movement can also have a wavy form. Its surface comprises a succession of hollows and crests of variable amplitude and rounded form, whose limits do not correspond to fractures in arrays. Each wave commonly displays a face covered with stylolites, indicating solution under tectonic pressure, and a face bearing

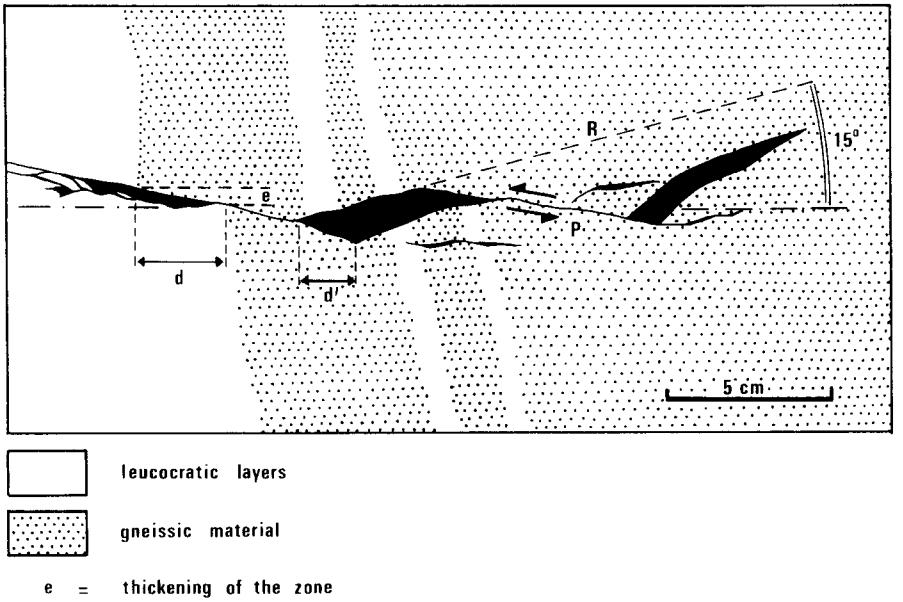

Fig. 3. Association of R-type and P-type fractures in gneiss of the Grandes Rousses Massif (French Alps). The offset of the leucocratic layers (d) is greater than that of the walls of the R-type fracture (d').

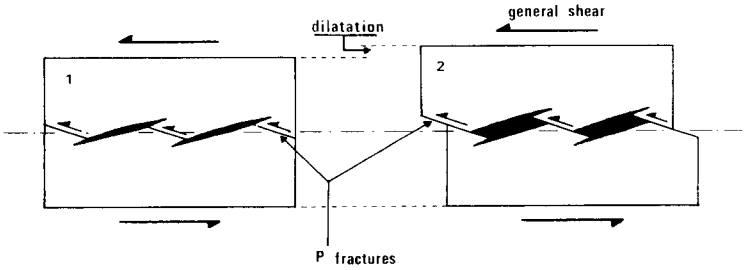

Fig. 4. P fractures oblique to the direction of shear. Slip on P fractures causes the tension fractures to open and thicken the shear zone.

crystal fibres that have grown parallel to the translation direction (Elliott 1976) in the gap created when the fault moved (Fig. 5).

Contrary to the situations illustrated in Figs. 1–3, there is no sliding on the right-stepping sides of the waves in Fig. 5 but imbrication of the two wall-rocks along these sides by a pressure solution process and corresponding deposition on the left-stepping sides of the waves. As a consequence of these processes the shear zone preserves its initial thickness.

The fault zones can take on very different forms and bring together several elements which are not always easy to identify; for example the angle between T fractures and shear planes varies from 30 to 90° and hence it is possible to question whether they really are T fractures. In addition it is not possible to deduce from such observations a general picture of the way in which shear planes develop. The relative displacement of the walls, accompanied by sliding on one of the sets of elementary planes and dilatation of the fault zone, probably correspond to different mechanical conditions from those which give rise to a wavy fault zone without dilatation, but it is also possible that there is a complete range of intermediate types.

In an attempt to answer some of these questions, some direct shear-test experiments under constant normal stress were performed, the model being analogous to a fault zone involving dilatation (Fig. 4). It seems likely that this structure can develop when dilatation of the zone (by oblique sliding and/or material dilatancy) is not inhibited by a kinematic constraint. In this case the dilatation probably acts against a constant effective-normal stress which could be taken to represent the lithostatic load in the case of thrust faults.

The situation in which dilatation is impossible (specific experiments will be run soon) can be represented by a strike–slip fault. In this case, dilatancy takes place between two rigid wall-rocks and induces an increase in normal stress on the fault (Nur *et al.* 1973). The direct shear-test experiments worked out under constant normal stress were interpreted by reference to the work of many authors (e.g. Hill 1950, Hansen 1961, Morgenstern & Tchalenko 1967). I compare natural fracture patterns with those obtained experimentally and those predicted theoretically (Kutter 1971, Boudon 1976, Segall & Pollard 1980).

ANALOGUE MODEL OF A FAULT ZONE

Experimental method

The material used for the experiments was a periglacial varved clay, overconsolidated by a glacier about 150-m thick. The corresponding overconsolidation stress was probably of the order of 1.4 MPa. The overall mineralogical composition of the material was: calcite 28%, quartz 28%, feldspars 9%, illite 13% and chlorite 22%. The clays consisted of alternating parallel layers of pale and dark colours. The average water content of 17–19% measured during the experiments was very close to the saturation value (19%).

The direct-shear experiments performed with Casagrande-type boxes were carried out under different conditions: (a) in undrained conditions at a shear-strain rate of 1 mm min^{-1}, with vertical stresses of 0.5×10^{-1}–3.5×10^{-1} MPa, that is much less than the overconsolidation stress, on parallelepipedic samples of large dimensions (25 cm × 15 cm × 14 cm) and conventional dimensions (6 cm × 6 cm × 4 cm); and (b) in drained conditions at a shear-strain rate of 10 μm min^{-1} with the same vertical stresses and on samples of the same dimensions as in the undrained tests.

In all experiments the shear plane imposed by the box was horizontal and the bedding planes were vertical, parallel to the shearing direction in order to overcome, as far as possible, the influence of the primary planar fabric. Some experiments performed with the bedding

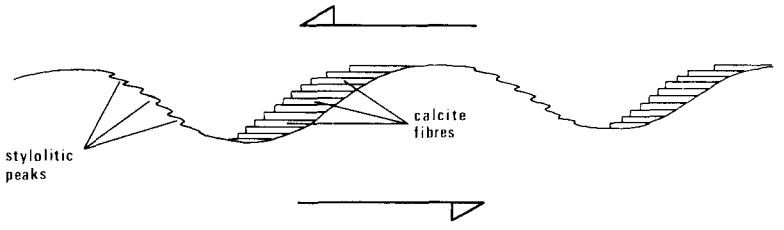

Fig. 5. Calcite fibres and stylolites on a wavy fault surface (after Elliott 1976, fig. 132). For explanation see text.

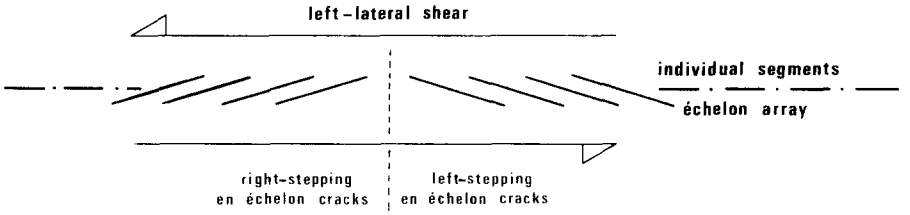

Fig. 6. Notation used in the experiments (after Segall & Pollard 1980).

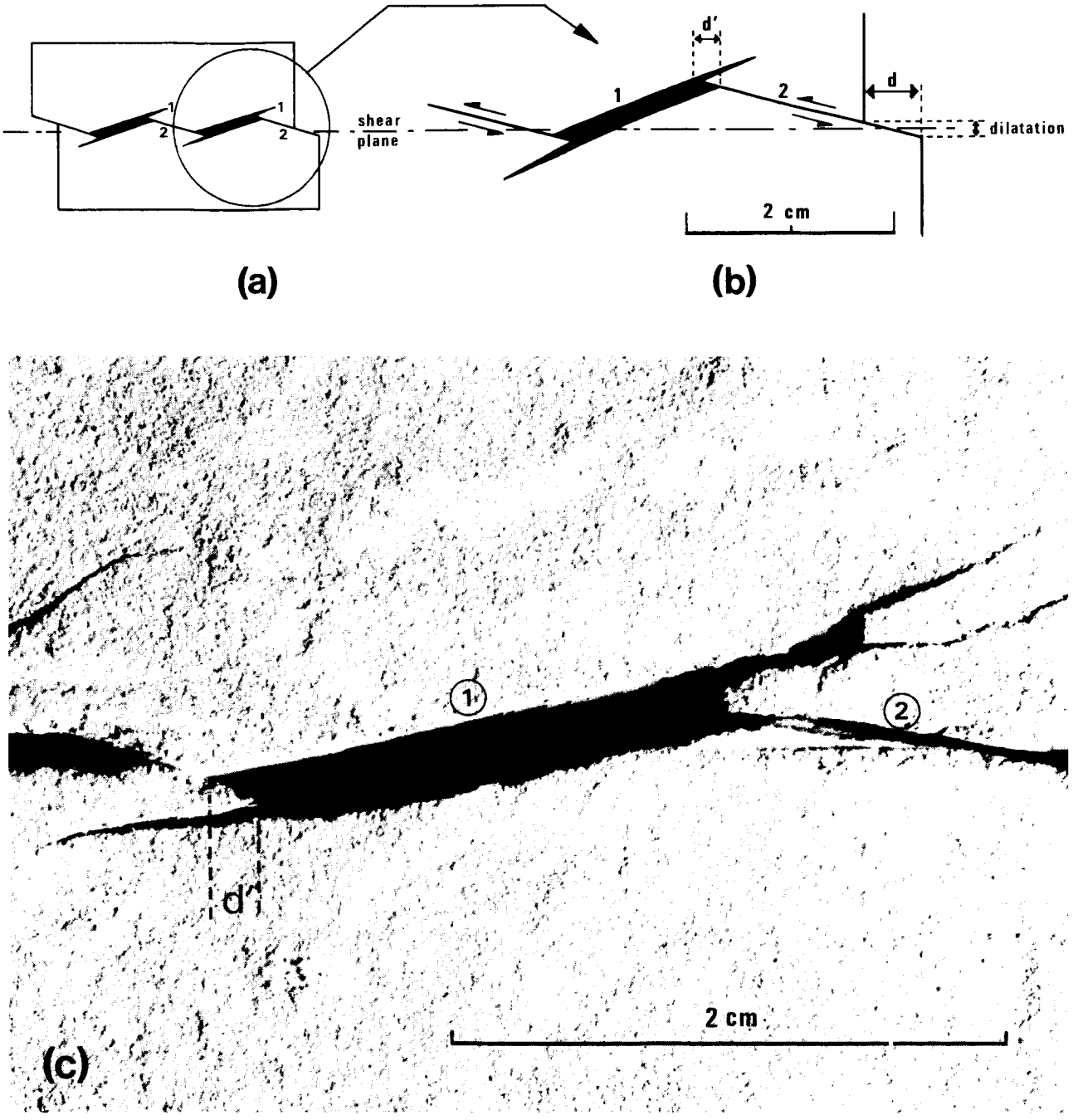

Fig. 7. (a) Types of experimentally produced ruptures: (1) individual primary fractures (right-stepping); (2) individual secondary fractures (left-stepping). (b) Detail of the circled section in (a): *d* displacement of the box margin, *d'* horizontal component of displacement on type (2) fracture. (c) Photograph of detail shown in (b).

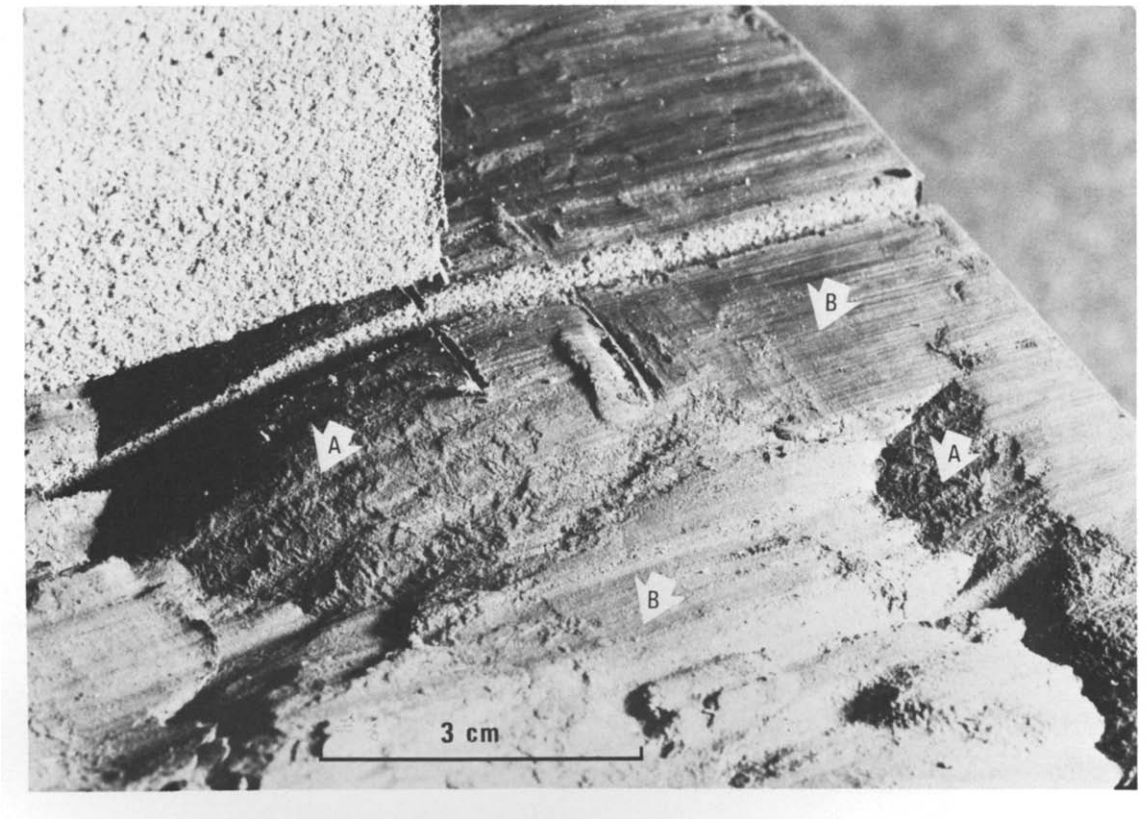

Fig. 9. Aspects of a general shear plane. Arrows labelled A show primary fracture planes and arrows labelled B show secondary fracture planes.

plane perpendicular to the shearing direction were not continued because horizontal planes were obtained through brittle fracture and there was no visible deflection of the bedding.

Experimental results

The conventional notation used by Segall & Pollard (1980) and given in Fig. 6 is employed here. The direct-shear experiments under drained and undrained conditions were carried out beyond rupture until the value of the shearing stress (τ) stabilized. After rupture, when the horizontal shearing plane imposed by the box was observed, it appeared to be composed of two sets of en échelon fractures on the left-lateral shear plane, one right-stepping, the other left-stepping.

The metal walls of the shearing boxes did not allow the different fractures to be observed while they formed; only the final result could be seen. However, the relative disposition of the two fracture types (Fig. 7) was reproduced in all experiments and it was observed that left-stepping fractures join with the right-stepping ones without cutting them. It is considered that this arrangement was adequate, given the small angle of their intersection (30°, see Fig. 7) to suggest the following order of events: the right-stepping fractures appeared first (primary fractures), then left-stepping fractures (secondary fractures) across the bridges of the intact material which separated the primary fractures.

The association of the two types of fractures brought about an effective separation of the two halves of the sample and allowed them to slide. The angles between the two types of planes and the horizontal shear plane (Fig. 8) allow the following observations. Primary and secondary fractures tend to be symmetrical with respect to the horizontal plane; this symmetry however seems more perfect in the case of the undrained models. The angles are very similar (8–10°) for low normal stresses (0.5×10^{-1} MPa). The angles tend to decrease when the stress normal to the shear plane increases in drained samples. On the contrary, in undrained samples, they tend to increase with an increase in the stress normal to the horizontal plane. Under undrained conditions the shear zone (composed of a few, well-developed fractures) has a greater thickness, with respect to the height of the sample, than under drained conditions, when it is thinner and composed of many short fractures (Fig. 8).

The primary fractures generally formed a single and well-organized set of planes. Their surfaces displayed a matt and finely granular texture indicating that they were created at least in part by traction (Fig. 9, arrow A).

The secondary fractures were more wavy and were commonly attached to the primary fracture by a sector which was nearly horizontal. The surfaces of these fractures were shiny, darker (damp), and had grooves demonstrating that there had been significant friction during displacement (Fig. 9, arrow B).

If we accept, as proposed above, the order of development of the fractures in the two systems of arrays, it seems that left-lateral shear first produced right-stepping en échelon tension fractures, and then by rupture of the bridges which joined them, secondary left-stepping shear planes which directed the relative sliding between the two halves of the sample and transformed the left-lateral horizontal movement transmitted by the two half-boxes into a left-oblique movement. After this sliding the primary fractures opened and their tips separated by a value d' (Figs. 7b & c).

However, the primary fractures were probably shear fractures, as will be argued in the mechanical interpretation section. Thus the general shearing along the horizontal plane was revealed through an array of primary shear fractures which opened in traction due to sliding on the secondary shear fractures.

The sliding on the secondary fractures was accompanied by a change in volume of the clay material in their neighbourhood. This change was observed when, after the experiment, the two halves of the sample were replaced one on top of the other, in a position corresponding to a displacement (d) of zero. It was then seen that it was impossible to re-imbricate the fractures in such a way that there was no space between them ($d' < d$, Fig. 10). Thus it was necessary to admit that sliding with friction on the secondary fractures was locally accompanied by a decrease in volume of material and that there was a transpression zone (Harland 1971, Lowell 1972) associated with a transtension zone represented by the open primary fracture.

The left-lateral movement oblique to the horizontal plane, on the secondary fractures likewise resulted in the dilatation of the samples and caused the rise to the left of the upper wall (Fig. 7b). The dilatation imparts on the piston a continuous upward movement, becoming weaker as the applied normal stress is increased (Fig. 11).

MECHANICAL INTERPRETATION OF THE CREATION OF THE FRACTURES IN THE SHEAR ZONE

In the experiments, neither the primary fractures nor the secondary ones coincided with the horizontal shear plane imposed by the box; the following interpretation takes into account these facts. In the interpretation, proposed by Hill (1950) and Hansen (1961) and restated by Morgenstern & Tchalenko (1967), Wallace (1973) and Vialon *et al.* (1976), the values of σ_{na} and τ_a obtained in the drained direct shear tests measure the effective stresses on the horizontal shear plane, which is not the rupture plane but that on which the peak shear stress applies (thus $\tau_a = \tau_{max}$ and σ_1 is at 45° to the horizontal plane). Hence in the Mohr space the point (σ'_{na}, τ_a) is the point whose value on the ordinate is greatest for a circle with the centre (σ'_{na}, 0) (Fig. 12). The value of σ'_1 and σ'_3 can thus be determined simply. As a result the effective major principal stress (σ'_1) in the shear zone makes an angle of 45° with the horizontal shear plane. The Mohr envelope is tangent to the circle of centre (σ'_{na}, 0) at a point which represents the rupture plane (Fig. 12a). The

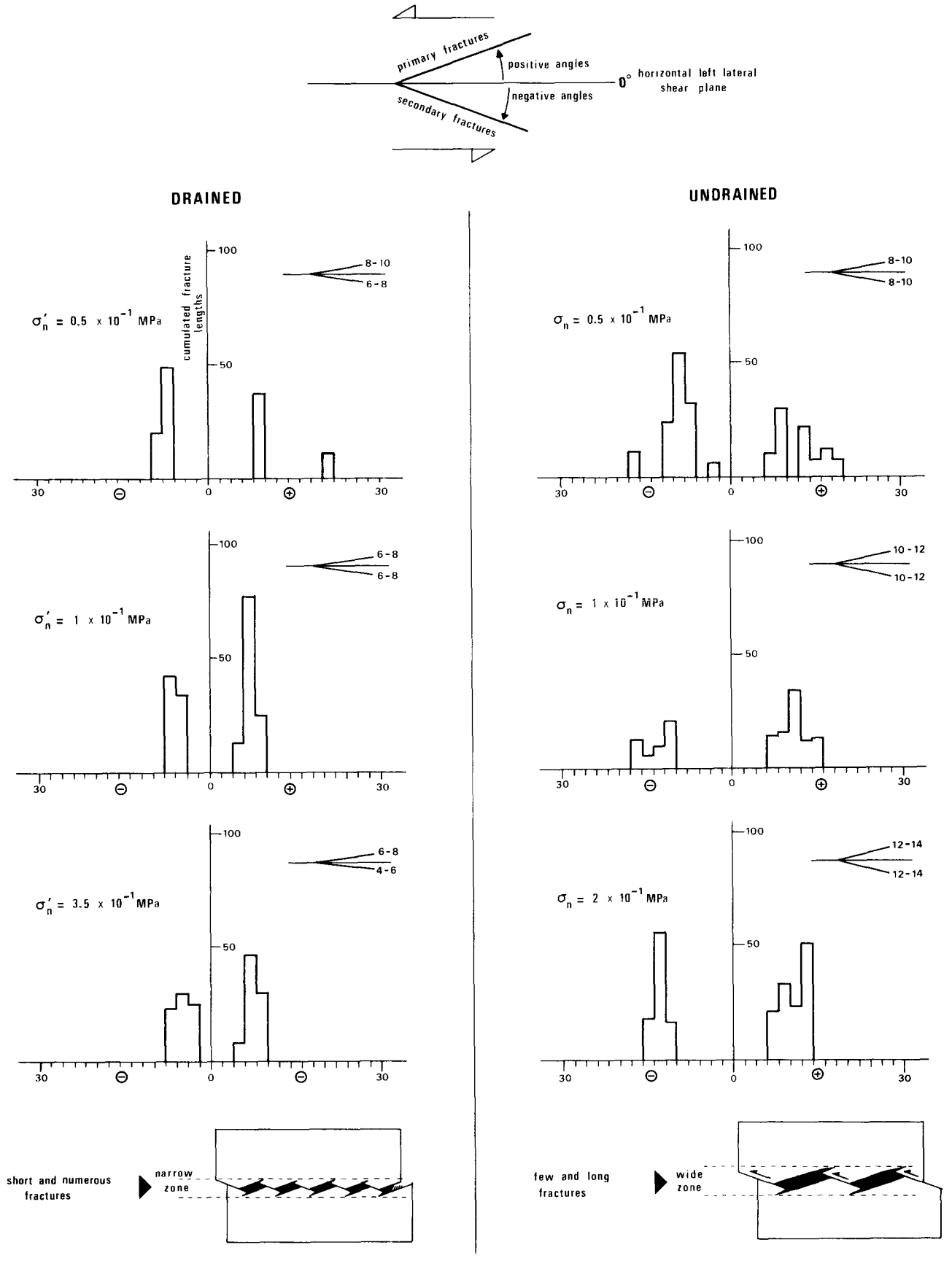

Fig. 8. Angular relationships between the two types of fractures and the horizontal shear plane, under drained and undrained conditions.

angle between the normal to the fracture surface and the direction of the major principal stress determines a right-stepping facet in relation to the horizontal shear plane (Fig. 12b). This position corresponds to that of the primary fractures observed in the experiments.

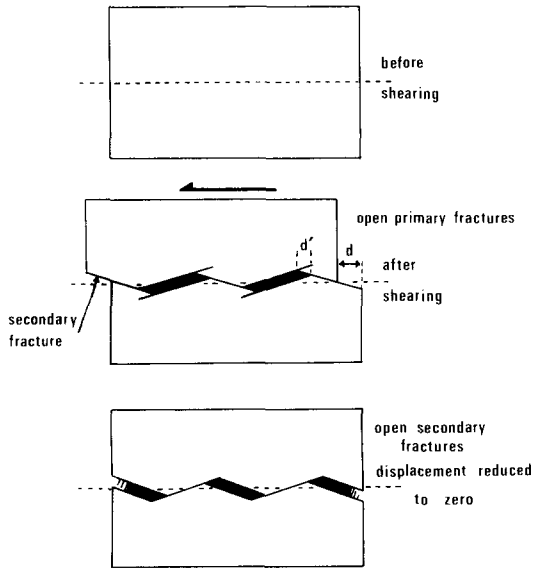

Fig. 10. Experimental evidence for the variation in volume of material along secondary fractures.

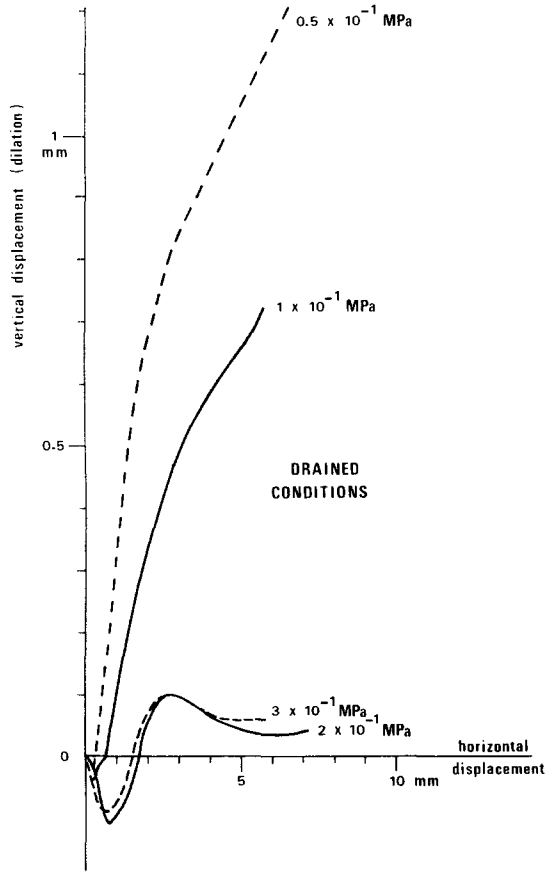

Fig. 11. Dilatation of the samples by the vertical displacement of the piston in proportion to the normal applied stress.

Creation of the primary fractures

By employing non-adjusted peak resistances in terms of effective stresses, yielded by the drained direct-shear experiments, the line given in Fig. 12(a) ($\phi_r = 20°$) was obtained by Terzaghi's construction so as to give an inclination of the order of 10° of the primary fractures with respect to the horizontal shear plane (Fig. 12b). This situation corresponds to the orientation of the primary fractures in the drained models (Fig. 7), see also Tchalenko 1970.

Creation of the secondary fractures

If new fractures appear in another direction, the stresses corresponding to the part of the curve (τ/displacement) which follows the peak stress, should reflect the development and the position of the secondary fractures. The stresses thus determined are those which act on the horizontal plane in the intact material separating the primary fractures and where the secondary fractures are going to develop. For this to occur the intact material should be stressed to its own peak resistance τ_2 ($\tau_2 > \tau_a > \tau_{residual}$), even if at this moment the curve reflects an unstable rupture of the sample (Fig. 13).

If the normal and tangential stresses on the horizontal plane are known it is possible to construct a Mohr circle tangent to the envelope and passing through the point (σ'_{na}, τ_2) representing these stresses. The angle determined from Fig. 13(a) gives the orientation of the new $\sigma'_1{}^*$ with respect to the horizontal plane. The angle Θ'_r gives the orientation of the secondary rupture plane with respect to the new $\sigma'_1{}^*$.

Those fractures which occur in a left-stepping position with respect to the horizontal shear plane and make with it an angle of 10° (Fig. 13b) are similar to the secondary fractures observed in the clay models (Fig. 7).

Other elements supporting the interpretation

Shear models. The interpretation proposed above implies that at first the major principal stress (σ'_1) in the shear zone makes an angle of 45° with the horizontal shear zone (Fig. 12). This geometric consequence of the basic hypothesis seems to be confirmed by the calculations carried out by Kutter (1971) on models of direct-shear tests on elastic media (Fig. 14a), and Boudon (1976) for indirect shear of a cover by a basement block indenter (Fig. 14b).

Prediction of secondary fracture development by computation. A different approach to the development of second-generation fractures between pre-existing fractures in an array is given by Segall & Pollard (1980). These authors discuss different cases of fractures in arrays (right-stepping and left-stepping) with a far-field state of stress where σ_1 makes an angle of 30° with the direction of the individual fractures (a situation analogous to that shown in Fig. 13b). The orientations of the shearing and extension directions likely to break the bridges between the pre-existing cracks were computed as a function of their length (a), separation (s) and step

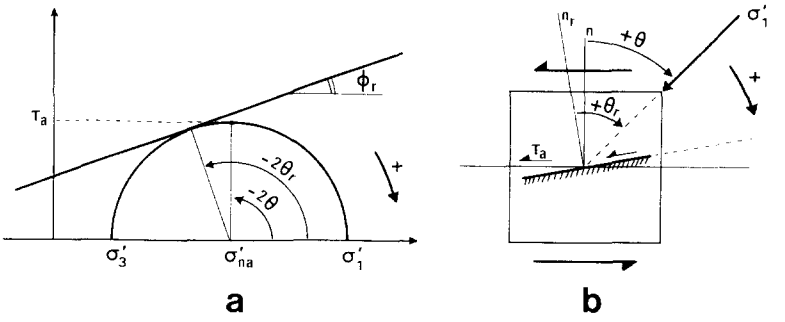

Fig. 12. Interpretation of the direct shear test following Morgenstern & Tchalenko (1967). Development of primary fractures. (a) Mohr's circle interpretation of rupture: τ_a and σ'_{na}, respectively tangential and normal effective stresses measured in the experiments; σ'_1 and σ'_3 maximum and minimum principal effective stresses; θ_r, angle between the outer normal of the rupture plane and the σ'_1 direction; ϕ_r, angle of internal friction of the material. (b) Attitude of the rupture plane with respect to the horizontal one. For explanation see text.

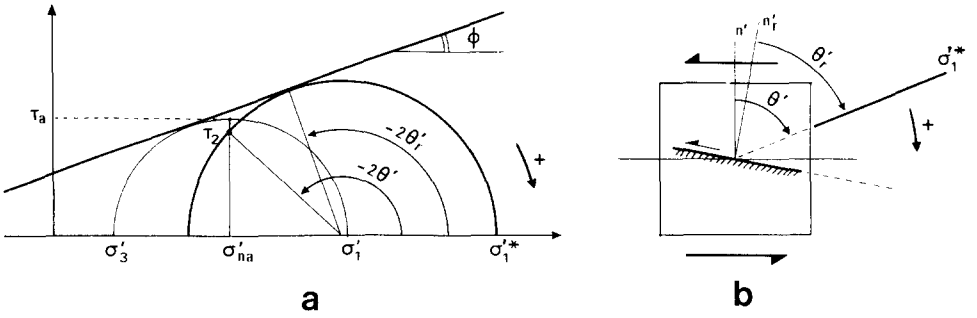

Fig. 13. Conditions for creating secondary fractures. (a) Mohr's circle interpretation of secondary fractures: τ_2, tangential post-peak stress on the horizontal plane; σ'^*_1, maximum principal stress within the intact material between two primary fractures; θ_r, angle between the outer normal of the secondary rupture plane and the σ'^*_1 direction; θ', angle between the outer normal of the horizontal plane and the σ'^*_1 direction. (b) Attitude of the secondary rupture plane with respect to the horizontal one. For explanation see text.

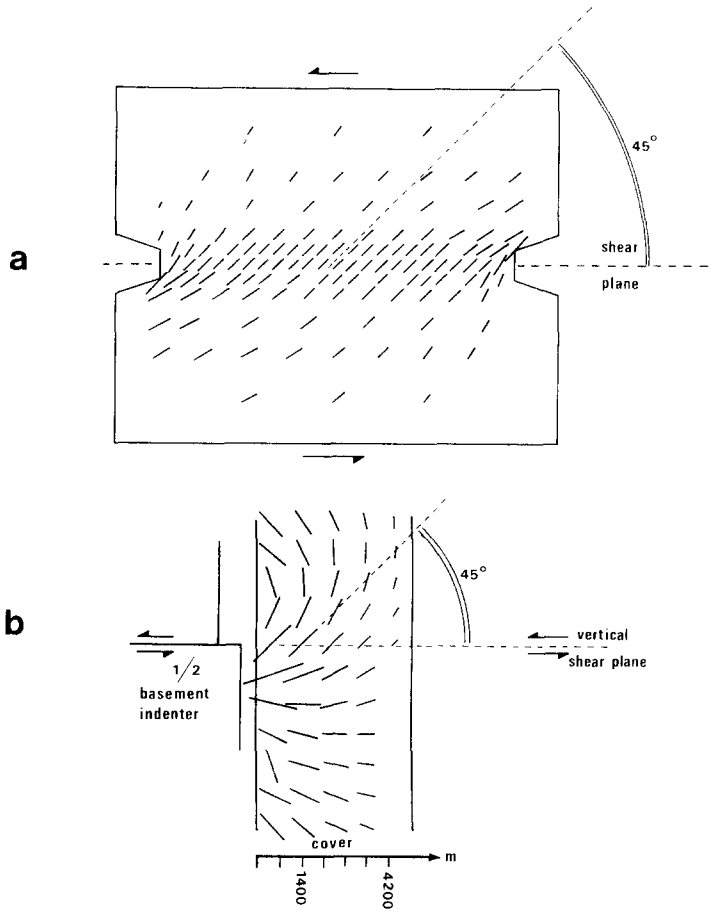

Fig. 14. (a) Reorientation of σ_1 at 45° to the shear plane in the central part of a computed model (after Kutter 1971, fig. 5). (b) Reorientation of σ_1 at 45° to the shear plane above a basement indenter (after Boudon 1976, fig. 49).

(d). Figure 15 shows the results computed for two cases with the following characteristics: $\sigma_1^\infty = 5\sigma_3^\infty$, σ_1 at 30° to the direction X, separation $2s$ positive, $d/a = 0.1$, $s/a = 0.06$.

In the case of right-stepping primary fractures in a left-lateral shear, one of the computed shear planes (heavy line in Fig. 15d) makes an angle of about 15° with the primary fractures and corresponds to the secondary fractures obtained in the clay experiments (Fig. 7b). It should also be noted that in the zone of probable development of the second-generation plane (Fig. 15c) there is a reorientation of σ_1 which corresponds to the situation represented in Fig. 13(b).

The calculation also takes account of the increase in the normal stresses on the pre-existing en échelon fractures and the decrease of the tangential stresses in the material which separates them. The effect of this is to inhibit sliding on the primary planes, implying that for deformation to continue the bridges must break along the second-generation planes (Fig. 15d). The evolution of such a situation is analogous to that which was inferred from the clay models (Fig. 7).

In the case of left-stepping first-generation fractures on a left-lateral shear (Fig. 15a & b) an inferred reorientation of σ_1 is observed between the cracks in the opposite sense to that which is depicted in Fig. 15(c). It should

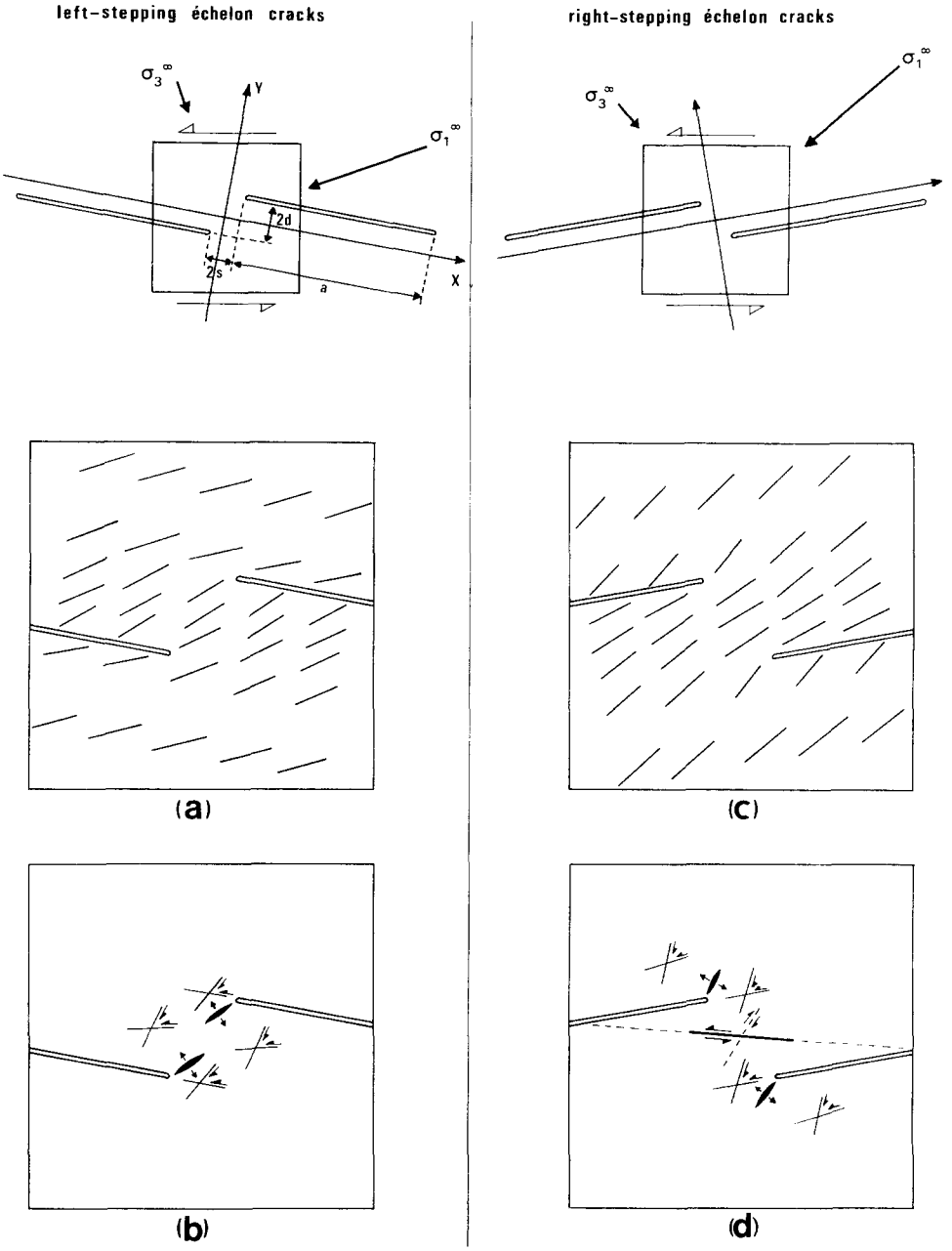

Fig. 15. (a) and (c). Reorientation of σ_1 between en échelon fractures. (b) and (d). Computed second-generation tension and shear cracks. In (d) the heavy line marks the position of a secondary shear plane similar to those obtained in the clay models (Fig. 7b). In (b), the tension cracks are located similar to those of the open fractures of the dominoes illustrated in Fig. 1.

also be noted that the expected positions of the second-generation extension cracks make an angle of 50° with the direction of the individual fractures in the array.

COMPARISONS BETWEEN NATURAL STRUCTURES AND THE PHYSICAL OR COMPUTED MODELS

The different structures associated with a fault zone should correspond to the different conditions determining sliding in the zone, with or without shearing of the sides. The method used in the experiments described in this paper allows only some situations to be specified but it seems however that the conditions for the development of certain structures can be better understood.

Analogies with computed models

In a left-lateral displacement zone the evolution of the sets of fractures predicted by calculation (Figs. 15b & d) gives rise to patterns analogous to those observed in natural examples (Figs. 1–3).

In the situation illustrated in Fig. 15(b) (where the angle between the primary fractures and the secondary tension cracks is 50°) it is possible to obtain by sliding on the primary fractures a pattern analogous to that shown in Fig. 1.

In the situation illustrated in Fig. 15(a) (where the angle between primary and secondary fractures has a value of 20–30°), the pattern obtained is identical to that shown in Figs. 2 and 3.

The left-lateral sliding on the left-stepping fractures results in both cases in the opening of the other set of fractures (i.e. the creation of fibrous fillings in the dominoes) and a thickening of the shear zone.

Analogies with clay models

The clay models can now be compared to the natural examples illustrated in Figs. 2 and 3. The following list catalogues the common features observed.

Primary and secondary fractures are disposed in arrays with opposite senses of stepping with respect to the general shear direction of the fault zone. This could signify that σ_1 in the interior of the fault zone rotates, for example under the effect of dilatation. The angles between the primary and secondary fractures are less than 45°; 20° for the models, 20–40° for the natural examples. The left-lateral slip on the secondary fractures resulted in a thickening of the shear zone, which constitutes a part of the vertical dilatation of the samples (Fig. 8), and the development of zones of transpression with volume variations localized around the fractures. This sliding caused the opening of primary fractures which then behaved like zones of transtension.

The great similarity between the natural structures and the experimentally produced fractures suggests that the interpretation given in Fig. 4 should be modified: the right-stepping primary fractures, which were considered as T fractures, correspond more probably to shear fractures (Fig. 12b) that open only during sliding on the secondary fractures.

CONCLUSIONS

The type of brittle–ductile shear zone described in this paper is largely represented in the higher levels of the crust. It is generally formed through the connection of several sets of fractures in an array. Commonly, arrays are separated into two sets, one right-stepping, the other left-stepping, whose interconnection gives the resulting discontinuity a broken or wavy form. Comparison between structures modelled during experiments, simulated by calculation and observed in nature, permits the following conclusions to be formulated.

The development of elementary fractures in array brings about a systematic reorientation of the stresses in the interior of the shear zone. The sense of rotation of the stresses is dependant on the order of development of the different types of elementary fractures: in a left-lateral shear, primary right-stepping fractures bring about a right-handed rotation of the major principal stress, while left-stepping primary fractures cause a left-handed rotation of the major principal stress.

It seems that the angles between left-stepping and right-stepping fractures are different according to their order of development. Between right-stepping primary fractures and the left-stepping secondary fractures which join them, the angles do not seem to exceed 20–30° (i.e. tailed dominoes). Between primary left-stepping fractures and secondary right-stepping ones the angle can reach 50° (the secondary tension fracture is more transverse to the shear zone than the primary fracture).

However, in both of these configurations the value of the angles varies and the reasons for this are not understood, nor are those which control the first development of left-stepping rather than right-stepping fractures.

The relative displacement on either side of broken or wavy discontinuous surfaces can occur in two ways. First, by sliding on one of the sets of elementary discontinuities and the subsequent opening of the other set within which crystal fibres lie parallel to the direction of sliding. This oblique sliding with respect to the shear zone gives rise to a thickening of the zone, that is a process equivalent to dilatancy. As the empty spaces are filled there is an increase in volume. This change can be compensated at least in part, by a volume decrease such as the one observed in the clay models along the fractures on which sliding occurred. This can possibly be explained by pressure–solution processes, with migration of ions along the fracture planes or diffusion across the matrix and deposition in the empty spaces. Second, by pressure–solution without sliding along a set of fractures and by deposition of crystal fibres in the planes of the other set, parallel to the fault zone, thus, maintaining a constant thickness along the deformed zone.

Acknowledgements—The original version of the paper was read by P. Choukroune, D. Fabre and P. Vialon. Their valuable suggestions are gratefully acknowledged. I thank particularly Dr. P. L. Hancock for his comments and constant correction of style and syntax.

REFERENCES

Bodou, P. 1972. Etude de la tectonique de la côte basque entre Hendaye et Bidart. Diplôme d'Etudes Supérieures, Strasbourg.

Boudon, J. 1976. Application de la méthode des éléments finis à l'approche mécanique d'un phénomène tectonique, le poinçonnement (cas d'une couverture sédimentaire déformée par un mouvement d'un compartiment de socle). Thèse Docteur Ingénieur Grenoble.

Delair, J. 1977. Fracturation des roches calcaires. Thèse 3ème Cycle, Montpellier.

Durney, D. W. & Ramsay, J. G. 1973. Incrementral strains measured by syntectonic crystal growths. In: *Gravity and Tectonics* (edited by De Jong, K. A. & Scholten, R.). Wiley, New York, 67–96.

Elliott, D. 1976. The energy balance and deformation mechanisms of thrust sheets. *Phil. Trans. R. Soc.* **283A**, 289–312.

Fabre, D. & Robert, J. P. 1975. Analyse expérimentale des ruptures de la couverture liées à un mouvement décrochant du socle et applications. *Ann. Soc. géol. N.* **95**, 175–182.

Hancock, P. L. 1972. The analysis of en-echelon veins. *Geol. Mag.* **109**, 269–276.

Hansen, B. 1961. Shear box tests on sand. *Proc. 4th. Int. Conf. Soil Mech.* **1**, 127–131.

Harland, W. B. 1971. Tectonic transpression in Caledonian Spitzbergen. *Geol. Mag.* **108**, 27–42.

Hill, R. 1950. *The Mathematical Theory of Plasticity*. Clarendon Press, Oxford.

Kutter, H. K. 1971. Stress distribution in direct shear test samples. *Proc. Symp. Soc. Int. Mecanique des Roches*, Nancy.

Lowell, J. D. 1972. Spitzbergen Tertiary orogenic belt and the Spitzbergen fracture zone. *Bull. geol. Soc. Am.* **83**, 3091–3102.

Morgenstern, N. R. & Tchalenko, J. S. 1967. Microscopic structures in kaolin subjected to direct shear. *Géotechnique* **17**, 309–328.

Nur, A., Bell, L. & Talwani, P. 1973. Fluid flow and faulting: a detailed study of the dilatancy mechanism and premonitory velocity changes. In: *Proc. Conf. on Tectonic Problems of the San Andreas Fault System* (edited by Kovach, R. & Nur, A.). Stanford Univ. Publ. **13**, 391–404.

Robert, I. 1979. Etude des mécanismes de plissement d'une série stratifiée dans une zone de cisaillement: exemple de la côte basque. Thèse 3ème Cycle, Grenoble.

Segall, P. & Pollard, D. D. 1980. Mechanics of discontinuous faults. *J. geophys. Res.* **85**, 4337–4350.

Spörli, K. B. & Anderson, H. J. 1980. Paleostress axes from mineral striations in faulted Mesozoic basement, Auckland, New Zealand. *N.Z. Jl Geol. Geophys.* **23**, 155–166.

Tchalenko, J. S. 1970. Similarities between shear zones of different magnitudes. *Bull. geol. Soc. Am.* **81**, 1625–1640.

Tchalenko, J. S. & Ambraseys, N. N. 1970. Structural analysis of Dasht-e Bayaz (Iran) earthquake fractures. *Bull. geol. Soc. Am.* **81**, 41–60.

Vialon, P., Ruhland, M. & Grolier, J. 1976. *Elements de Tectonique Analytique*. Masson, Paris.

Vialon, P. 1979. Les déformations continues–discontinues des roches anisotropes. *Eclog. geol. Helv.* **72**, 531–549.

Wallace, R. E. 1973. Surface fracture patterns along the San Andreas fault. In: *Proc. Conf. on Tectonic Problems of the San Andreas Fault System* (edited by Kovach, R. & Nur, A.). Stanford Univ. Publ. **13**, 248–250.